



Correlation Between Neuromelanin-Sensitive MRI and ^{18}F -FP-CIT PET in Early-Stage Parkinson's Disease: Utility of a Voxel-Wise Analysis by Using High-Spatial-Resolution MRI

Seongbeom Park^a

Young Hee Sung^b

Woo Ram Kim^c

Young Noh^b

Eung Yeop Kim^d

^aHeuron Co., Ltd, Incheon, Korea

^bDepartment of Neurology,
Gil Medical Center, Gachon University
College of Medicine, Incheon, Korea

^cNeuroscience Research Institute,
Gachon University, Incheon, Korea

^dDepartment of Radiology,
Samsung Medical Center,
Sungkyunkwan University
School of Medicine, Seoul, Korea

Background and Purpose The correlation between dopamine transporter (DAT) imaging and neuromelanin-sensitive magnetic resonance imaging (NM-MRI) in early-stage Parkinson's disease (PD) has not yet been established. This study aimed to determine the correlation between NM-MRI and DAT positron-emission tomography (PET) in patients with early-stage PD.

Methods Fifty drug-naïve patients with early-stage PD who underwent both 0.8-mm isovoxel NM-MRI and DAT PET were enrolled retrospectively. Using four regions of interest (nigrosome 1 and nigrosome 2 [N1 and N2] regions) from a previous study, the contrast ratios (CRs) of 12 regions were measured: N1, N2, flipped N1, flipped N2, combined N1 and N2, and whole substantia nigra pars compacta [SNpc] (all on both sides). The clinically more affected side was separately assessed. The standardized uptake value ratios (SUVRs) were measured in the striatum using DAT PET. A partial correlation analysis was performed between the SUVR and CR measurements.

Results CR of the flipped left N1 region was significantly correlated with SUVR of the right posterior putamen ($p=0.047$), and CR values of the left N1 region, left N2 region, flipped right N1 region, and combined left N1 and N2 regions were significantly correlated with SUVR of the left posterior putamen ($p=0.011, 0.038, 0.020, \text{ and } 0.010$, respectively). SUVR of the left anterior putamen was significantly correlated with CR of the left N2 region ($p=0.027$). On the clinically more affected side, the CR values of the N1 region, combined N1 and N2 regions, and the whole SNpc were significantly correlated with SUVR of the posterior putamen ($p=0.001, 0.024, \text{ and } 0.021$, respectively). There were significant correlations between the SUVR of the anterior putamen and the CR values of the N1 region, combined N1 and N2 regions, and whole SNpc ($p=0.027, 0.001, \text{ and } 0.036$, respectively).

Conclusions This study found that there were significant correlations between CR values in the SNpc on NM-MRI and striatal SUVR values on DAT PET on both sides in early-stage PD.

Keywords Parkinson's disease; neuromelanin-sensitive MRI; dopamine transporter imaging.

Received April 6, 2022

Revised July 29, 2022

Accepted July 30, 2022

Correspondence

Eung Yeop Kim, MD
Department of Radiology,
Samsung Medical Center,
Sungkyunkwan University
School of Medicine,
81 Irwon-ro, Gangnam-gu,
Seoul 06351, Korea
Tel +82-2-3410-1701
Fax +82-2-3410-0055
E-mail neuroradkim@gmail.com

INTRODUCTION

Dopamine transporter (DAT) imaging has been widely used to determine the presence or absence of nigrostriatal degeneration in patients with parkinsonism. Striatal uptake values on DAT imaging have been suggested to be correlated with the number of neuromelanin-containing dopaminergic neurons in the substantia nigra pars compacta (SNpc).^{1,2} However, the application of DAT imaging is restricted by its high availability, cost, and radiation

© This is an Open Access article distributed under the terms of the Creative Commons Attribution Non-Commercial License (<https://creativecommons.org/licenses/by-nc/4.0>) which permits unrestricted non-commercial use, distribution, and reproduction in any medium, provided the original work is properly cited.

exposure. In contrast, magnetic resonance imaging (MRI) is more accessible, does not involve exposure to ionizing radiation, and is often suggested for patients who present with parkinsonism to rule out structural pathologies in the brain.

Neuromelanin-sensitive MRI (NM-MRI) has been used to identify the loss of neuromelanin-containing dopaminergic neurons in the SNpc in patients with Parkinson's disease (PD).^{3,4} This use of NM-MRI is supported by a recent study finding that the signal intensity on NM-MRI was correlated with the neuromelanin concentration.⁵

Given the utility of NM-MRI, it would be better to observe significant correlations between the measures (either signal intensity ratio or volume) in the SNpc on NM-MRI and the striatal uptake values on DAT imaging. Two previous studies found that SNpc volumes measured on NM-MRI were significantly correlated with DAT activity,^{6,7} but these studies may have been limited by their inclusion of patients with both early- and advanced-stage PD. The ceiling effect may lead to unreliable DAT imaging results in the advanced stages of PD, and so it would therefore be better to include drug-naïve patients with early-stage PD when assessing the relationship between NM-MRI and DAT imaging. Another limitation of the previous studies was that they did not perform an analysis based on the striatum and SNpc subregions. A recent study conducted a subregion-based analysis using NM-MRI and DAT imaging.⁸ However, it only found a significant relationship on the clinically defined, more affected side. Moreover, a greater loss of signal intensity in the SNpc on the clinically less affected side was found in a substantial proportion of patients (~38%). Neuronal loss in PD occurs on both sides of the SNpc, although asymmetric involvement is distinctively observed in the early stages. The results of that study might therefore have not fully established the relationship between NM-MRI and DAT imaging. This lack of clarification about the relationship between NM-MRI and DAT imaging may be explained by the following factors: 1) the inclusion of patients with advanced-stage PD, and 2) the limited spatial resolution in the previous studies is prone to being affected by the partial-volume effect, which in turn leads to lower reliability.

A recent study recommended using thinner (1.5 mm) NM-MRI for voxel-wise analysis of the SNpc.⁹ It would therefore be better to conduct a similar study with both drug-naïve patients with early-stage PD and NM-MRI with a high spatial resolution. In the present study, we obtained both 0.8-mm isovoxel NM-MRI and DAT positron-emission tomography (PET) images from 50 patients with early-stage PD, and adopted the regions of interest (ROIs) in the SNpc that were recently identified in a voxel-wise analysis¹⁰ to determine if there was a significant correlation between the measures of NM-MRI and DAT imaging.

METHODS

Participants

This retrospective study, which was approved by the Institutional Review Board of Gachon University Gil Medical Center (IRB no. GCIRB2021-177), enrolled 46 out of 50 patients with PD who were assessed in a recently reported study.¹⁰ All participants gave informed consent. The four patients were excluded because their raw data from N-3-fluoropropyl-2 β -carbomethoxy-3 β -(4-iodophenyl) nortropane PET (¹⁸F-FP-CIT PET) were unavailable. We therefore retrospectively recruited four patients with PD (maintaining the sex ratio [one female patient] and age range compared with those of the four excluded patients). All of the patients had been diagnosed with PD between January 2018 and April 2020. Both MRI and ¹⁸F-FP-CIT PET of the head were obtained for the initial diagnosis. Motor symptoms were assessed by an experienced neurologist using the Hoehn and Yahr scale¹¹ and Unified Parkinson's Disease Rating Scale (UPDRS).¹² Clinical laterality of motor symptoms was considered to be present when the UPDRS III scores differed between the right and left sides. For cases without clinical laterality, the side with a lower standardized uptake value ratio (SUVR) of the posterior putamen on ¹⁸F-FP-CIT PET was considered to have been affected more. Only drug-naïve patients with early-stage PD (Hoehn and Yahr scale score ≤ 2.5) were included. Ninety-six healthy subjects were enrolled to create templates of unbiased NM-MRI and susceptibility map-weighted MRI (SMwI) data. Healthy subjects were participants of the Environmental Pollution-Induced Neurological Effects study, which involved a community population.¹³ Of those 96 healthy subjects, 50 age- and sex-matched subjects were chosen to determine the areas with significant differences in the SNpc through a voxel-wise analysis.

Imaging data acquisition

MRI was performed using a 3-T scanner with a 32-channel coil (Skyra, Siemens Healthineers, Forchheim, Germany). Whole-brain sagittal three-dimensional (3D) magnetization prepared rapid gradient echo (MP-RAGE) imaging was first obtained with the following parameters: repetition time (TR), 1,800 ms; echo time (TE), 3 ms; inversion time, 920 ms; matrix 256 \times 256; field of view (FOV), 250 \times 250; acceleration factor, 2; and acquisition time, 3 min and 35 s.

Oblique axial 3D multiecho gradient-recalled echo (GRE) imaging was obtained parallel to the plane from the posterior commissure and the top of the pons, which was localized using sagittal MP-RAGE imaging. The parameters of the 3D multiecho GRE imaging were as follows: TR, 48 ms; minimum TE, 14.38 ms; echo train length, 3; echo spacing, 12.3 ms; ma-

trix 384×384; FOV, 192×192 (100% phase resolution); slice thickness, 1 mm; number of slices, 32; acceleration factor, 2; and acquisition time, 4 min and 46 s.

Both magnitude and phase multiecho GRE images were used to reconstruct quantitative susceptibility mapping (QSM) using the iterative least-squares method. The SMwI images were reconstructed while using the QSM as a mask. This approach further enhanced the susceptibility contrast and improved the visualization of the nigrosome regions. Additional details for reconstructing SMwI can be found elsewhere.^{14,15}

T1-weighted 3D sampling perfection with application-optimized contrast using different flip angle evolutions (SPACE) imaging was obtained at the same imaging plane as multiecho GRE imaging, with the following parameters: TR, 900 ms; TE, 4.8 ms; echo spacing, 4.76 ms; echo train duration, 338 ms; variable flip angle; delay alternating with nutation for tailored excitation (DANTE) preparation to improve SNpc delineation;¹⁶ matrix 288×288; FOV, 230×230 (100% slice/phase resolution); slice thickness, 0.8 mm; number of slices, 208; acceleration factor, 2 (controlled aliasing in parallel imaging results in higher acceleration); and acquisition time, 5 min and 12 s. T1-weighted SPACE imaging with DANTE preparation was used in this study because it allowed high-spatial-resolution images to be obtained more rapidly, which has been shown to have a comparable diagnostic performance to GRE imaging with magnetization transfer.¹⁶

¹⁸F-FP-CIT PET was obtained using a PET/CT (computed tomography) scanner (Biograph-6, Siemens, Erlangen, Germany). CT was performed from the vertex to the base of the skull (30 mAs, 120 kVp, and thickness of 3 mm). PET imaging data were collected in a 3D scanning mode with 40 slices (thickness of 3 mm) at 120 min after the administration of 5 mCi (185 MBq) of ¹⁸F-FP-CIT. The CT data were used for attenuation correction.

Image processing

To measure DAT availability, SUVR values at both the ROI and voxel levels were calculated using the following procedure: First, we spatially normalized the reconstructed ¹⁸F-FP-CIT PET image of each patient into a stereotaxic space using SPM12 software (<https://www.fil.ion.ucl.ac.uk/spm/>), based on the registration of the coregistered T1-weighted MP-RAGE image to the Montreal Neurological Institute (MNI) templates of T1-weighted images. We then extracted regional averages from each normalized ¹⁸F-FP-CIT PET image for each ROI. To define the ROI masks in the MNI space, we modified the Oxford-GSK-Imanova striatal¹⁷ and probabilistic cerebellar¹⁸ atlases in the FSL package (<https://fsl.fmrib.ox.ac.uk/fsl>). The substriatal ROIs included the posterior putamen, anterior putamen, posterior caudate nucleus, anterior caudate nu-

cleus, and ventral striatum (Fig. 1). The reference ROI was placed in the cerebellar gray matter. Finally, the SUVR values in the substriatal ROIs of each patient were calculated after normalizing the ¹⁸F-FP-CIT PET images with the average values of the cerebellar ROI.

Processing of the NM-MRI images was performed using Advanced Normalization Tools (<https://www.nitrc.org/projects/ants>, version 2.1.52-0). To calculate contrast ratios (CRs), all NM-MRI images were spatially normalized using the NM-MRI template, which was constructed in a recent study that involved patients with early-stage PD and healthy subjects.¹⁰ Two areas in each SNpc were found to have significant differences on NM-MRI, notably in the nigrosome 1 and nigrosome 2 (N1 and N2, respectively) regions, when these areas were overlaid on the SMwI template (Fig. 2A and B).¹⁰ Since the areas with significant differences were the N1 and N2 on both sides, they were defined as the nigrosome ROIs in this study. The accuracies of localizations of the N1 and N2 regions were assessed because the nigrosome regions (and N2 in particular) were relatively small (Supplementary Material in the online-only Data Supplement). We measured the CR values of four nigrosome ROIs (N1 and N2 regions in the bilateral SNpc) and two composite ROIs (combined N1 and N2 regions on each side of the SNpc) among our data set (Fig. 3). Since the left nigrosome ROIs were slightly larger than those on the right, right-left (horizontally) flipped ROIs were also created to measure the CR values (Fig. 2C; Supplementary

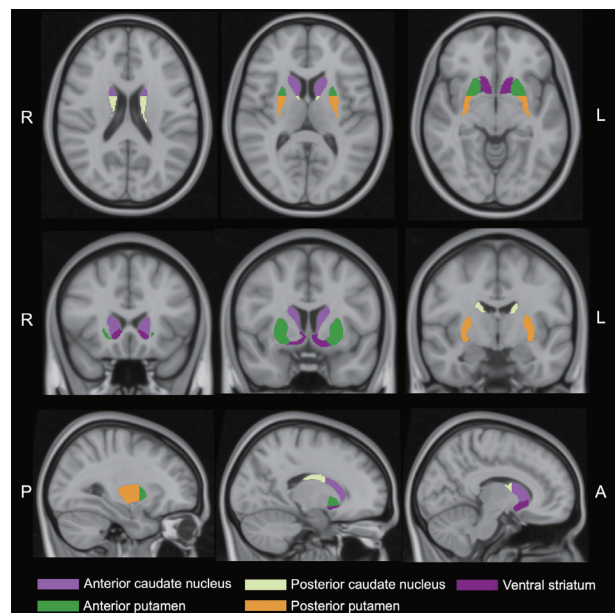


Fig. 1. The substriatal regions of interest consisted of the anterior caudate nucleus, posterior caudate nucleus, ventral striatum, anterior putamen, and posterior putamen. Each region is overlaid on the Montreal Neurological Institute template. R, right; L, left, A, anterior; P, posterior.

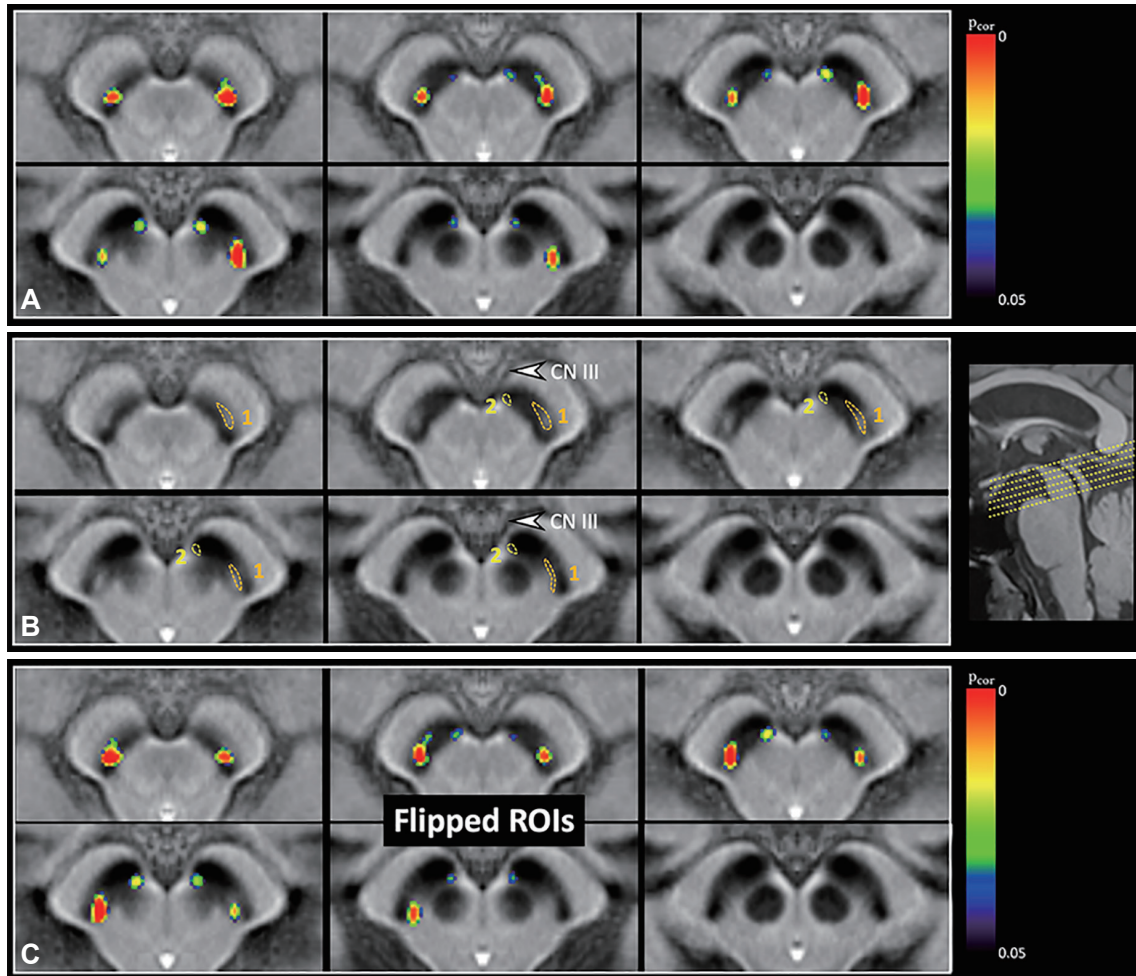


Fig. 2. Two areas in each side of the substantia nigra with significant differences on neuromelanin-sensitive magnetic resonance imaging (NM-MRI) between healthy subjects and patients with early-stage Parkinson's disease were determined and overlaid on a susceptibility map-weighted imaging template to determine their anatomical locations (A). These areas were noted in the nigrosome 1 and nigrosome 2 (N1 and N2, respectively) regions (orange and yellow dashed ovals, respectively) (B), which were defined as the regions of interest (ROIs) of N1 and N2. Right-left flipped ROIs were also created to measure the contrast ratios (C). CN III, third cranial nerve. Fig. 2A and B: adapted from Sung et al. *Hum Brain Mapp* 2021;42:2823-2832.¹⁰

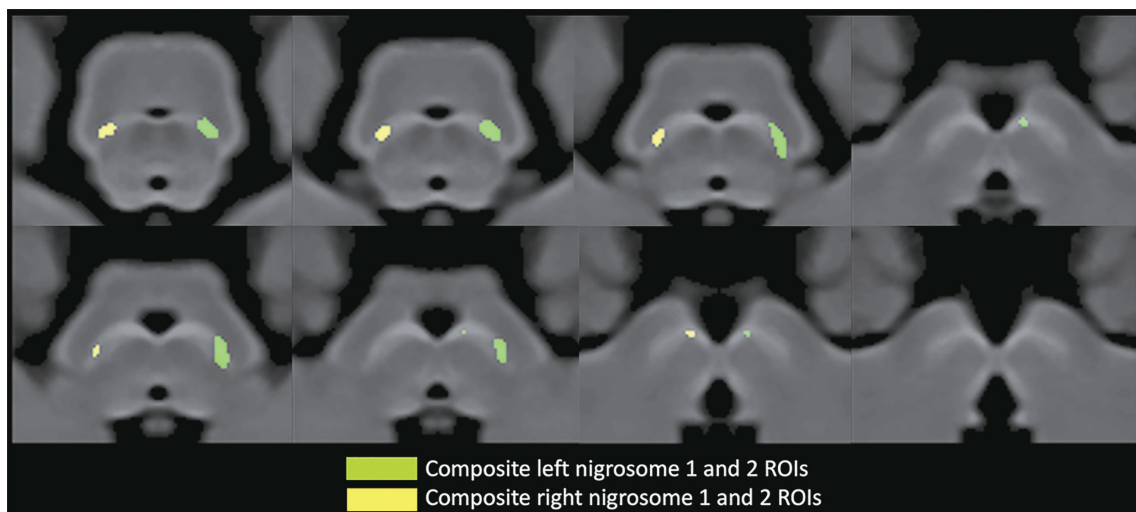


Fig. 3. The combined N1 and N2 regions of interest (ROIs) were defined as the composite N1 and N2 ROIs. The ROIs are depicted on the neuromelanin-sensitive MRI template.

Material in the online-only Data Supplement for use of the flipped ROIs). We also measured the CR values in the whole SNpc on both sides. The CR values of 12 ROIs were therefore assessed: N1, N2, flipped N1, flipped N2, combined N1 and N2, and whole SNpc (all on both sides). The sizes of the ROIs are listed in Supplementary Table 1 (in the online-only Data Supplement). The CR values measured on the clinically more affected side were assessed separately to determine if they were correlated with the SUVR values of the substriatal regions on ^{18}F -FP-CIT PET.

Statistical analysis

We conducted a partial correlation analysis after adjusting for age to test whether there were correlations between the SUVR values in each subregion on ^{18}F -FP-CIT PET and between the CR values of the ROIs in the SNpc on NM-MRI. The relationship between the clinical severity (UPDRS III score) and CR values of the ROIs in the SNpc on MRI was also assessed using a partial correlation analysis. Significance was set at $p < 0.05$. Statistical analyses were performed using SPSS (version 27, IBM Corp., Armonk, NY, USA).

RESULTS

Demographic and clinical characteristics

The 50 patients included 29 females. Five patients were left-handed, and the median age of all patients was 69 years (interquartile range [IQR]=58–78 years). The median disease duration was 6 months (IQR=3.3–12 months). The median UPDRS III score was 13 (IQR=9.3–22). Using the differences between the UPDRS III scores on the right and left, right and left dominant clinical laterality were determined in 29 and 14 patients, respectively (Supplementary Table 2 in the online-only Data Supplement). The clinical laterality of the remaining seven patients was determined using the SUVR of the posterior putamen on ^{18}F -FP-CIT PET, which revealed right and left dominant clinical laterality in four and three patients, respectively.

Correlations between the CR values of the SNpc on NM-MRI and SUVR values of the striatum on ^{18}F -FP-CIT PET

For the ROIs in the right SNpc, CR of the flipped left N1 region was significantly correlated with the SUVR of the right posterior putamen ($p=0.047$). No significant correlations were observed among the other regions (Table 1). The strengths of correlations between the CRs of the right N1 and N2 regions and the SUVRs of the right posterior putamen were modest, and not significant ($p=0.071$ and $p=0.068$, respectively).

For the ROIs in the left SNpc, the CR values of the left N1

region, left N2 region, the flipped right N1 region, and the combined left N1 and N2 regions were significantly correlated with the SUVR values of the left posterior putamen ($p=0.011$, $p=0.038$, $p=0.020$, and $p=0.010$, respectively). The SUVR of the left anterior putamen was significantly correlated with CR of the left N2 region ($p=0.027$). No significant correlations were found among the other regions (Table 1).

On the clinically more affected side, the CR values of the N1 region, combined N1 and N2 regions, and the whole SNpc were significantly correlated with the SUVR of the posterior putamen ($p=0.001$, $p=0.024$, and $p=0.021$, respectively). There were significant correlations between the SUVR values of the anterior putamen and the CR values of the N1 region, combined N1 and N2 regions, and whole SNpc ($p=0.027$, $p=0.001$, and $p=0.036$, respectively). In the other regions, there were no significant correlations between the CR values of the ROIs of the SNpc and the SUVR of the striatum on ^{18}F -FP-CIT PET (Table 2).

Correlations between the CR values of the SNpc on NM-MRI and clinical severity

There were no significant correlations between the CR values of all ROIs in the SNpc on NM-MRI and the UPDRS III scores on both sides (all $p > 0.05$).

The CR values of the whole SNpc and N1 and N2 regions, and their flipped regions, are listed in Supplementary Tables 3 and 4 (in the online-only Data Supplement). Box-and-whisker plots of the CR values in each SNpc region in patients with early-stage PD and healthy subjects are presented in the Supplementary Fig. 1 (in the online-only Data Supplement).

DISCUSSION

This study found significant correlations between SUVR values in the posterior putamen on ^{18}F -FP-CIT PET and CR values in the N1 regions of both sides of the SNpc in 50 drug-naïve patients with early-stage PD. In contrast to our results, a previous study only found a significant relationship on the clinically more affected side.⁸ The specific ROIs in the SNpc used in the present study to measure the CR values on the high-spatial-resolution NM-MRI template, which was derived from a voxel-wise analysis of 50 patients with early-stage PD and 50 healthy subjects, may also represent an advantage over the method employed in that previous study, where the ventral tier of the SNpc was arbitrarily defined on the NM-MRI template.⁸ However, our ROIs were more specific because their CR values for patients with PD differed significantly from those of healthy subjects. Different populations, the use of high-spatial-resolution NM-MRI, and the use of more-specific ROIs in the SNpc may have helped to yield better results.

When we determined the regions with significant differences between healthy subjects and patients with early-stage PD in the SNpc on NM-MRI in our previous study,¹⁰ we suggested that the larger number of right-handed patients may result

in size differences among the abnormal regions. However, it was still uncertain why the sizes of the areas with significant differences between the right and left N1 and N2 regions were different. We assumed that the smaller N1 and N2 regions on

Table 1. Correlations between CRs of the SNpc on NM-MRI and SUVRs of the striatum on ¹⁸F-FP-CIT PET on the right and left

	Anterior putamen	Posterior putamen	Anterior caudate nucleus	Posterior caudate nucleus	Ventral striatum
¹⁸ F-FP-CIT PET on the right					
N1 right					
Correlation	0.075	0.263	0.075	0.023	0.105
Significance	0.611	0.071	0.611	0.876	0.477
N2 right					
Correlation	0.229	0.266	0.067	-0.052	0.063
Significance	0.118	0.068	0.650	0.726	673
Flipped left N1					
Correlation	0.220	0.288	0.079	0.015	0.122
Significance	0.132	0.047*	0.594	0.917	0.408
Flipped left N2					
Correlation	0.203	0.189	0.124	-0.002	0.136
Significance	0.166	0.199	0.402	0.992	0.357
Combined right N1 and N2					
Correlation	0.183	0.257	0.067	0.061	0.099
Significance	0.213	0.078	0.653	0.680	0.502
Whole SNpc right					
Significance	0.198	0.150	0.051	-0.037	0.091
Correlation	0.178	0.308	0.731	0.805	0.539
¹⁸ F-FP-CIT PET on the left					
N1 left					
Correlation	0.260	0.363	0.186	0.155	0.135
Significance	0.074	0.011*	0.206	0.294	0.359
N2 left					
Correlation	0.320	0.300	0.238	0.057	0.240
Significance	0.027*	0.038*	0.103	0.701	0.101
Flipped right N1					
Correlation	0.231	0.335	0.177	0.167	0.129
Significance	0.113	0.020*	0.230	0.256	0.384
Flipped right N2					
Correlation	0.214	0.230	0.165	-0.011	0.120
Significance	0.145	0.116	0.261	0.943	0.417
Combined left N1 and N2					
Correlation	0.270	0.370	0.190	0.142	0.146
Significance	0.063	0.010	0.195	0.335	0.323
Whole SNpc left					
Correlation	0.251	0.280	0.188	0.088	0.168
Significance	0.085	0.054	0.201	0.552	0.254

**p*<0.05, statistical significance.

CR, contrast ratio; NM-MRI, neuromelanin-sensitive magnetic resonance imaging; N1, nigrosome 1; N2, nigrosome 2; SNpc, substantia nigra pars compacta; SUVr, standardized uptake value ratio; ¹⁸F-FP-CIT PET, N-3-fluoropropyl-2β-carbomethoxy-3β-(4-iodophenyl) nortropane positron-emission tomography.

Table 2. Correlations between CRs of the SNpc on NM-MRI and SUVRs of the striatum on ¹⁸F-FP-CIT PET on the clinically more affected side

	Anterior putamen	Posterior putamen	Anterior caudate nucleus	Posterior caudate nucleus	Ventral striatum
More-affected N1					
Correlation	0.319	0.464	0.057	0.029	0.024
Significance	0.027*	0.001*	0.701	0.843	0.869
More-affected N2					
Correlation	0.078	0.178	0.121	-0.046	0.141
Significance	0.599	0.225	0.412	0.755	0.341
More-affected combined N1 and N2					
Correlation	0.458	0.324	0.065	0.025	0.031
Significance	0.001*	0.024*	0.663	0.869	0.834
More-affected whole SNpc					
Correlation	0.304	0.332	0.162	0.059	0.134
Significance	0.036*	0.021*	0.272	0.690	0.363

* $p < 0.05$, statistical significance.

CR, contrast ratio; NM-MRI, neuromelanin-sensitive magnetic resonance imaging; N1, nigrosome 1; N2, nigrosome 2; SNpc, substantia nigra pars compacta; SUVR, standardized uptake value ratio; ¹⁸F-FP-CIT PET, N-3-fluoropropyl-2 β -carbomethoxy-3 β -(4-iodophenyl) nortropane positron-emission tomography.

the right on NM-MRI might not completely correspond to the histological (or pathological) N1 and N2. We therefore horizontally flipped the left N1 and N2 regions to the right SNpc, and calculated the CR values again. On the other hand, the left N1 and N2 regions might be bigger on NM-MRI than the histological (or pathological) N1 and N2. The right N1 and N2 regions on NM-MRI were therefore also flipped horizontally to the left, and the CR values were measured again. While the CR values of the left N1 region were significantly correlated with the SUVR values of the ipsilateral posterior putamen on ¹⁸F-FP-CIT PET, those of the right N1 region were not significantly correlated with the SUVR values of the ipsilateral posterior putamen. In contrast, the flipped left N1 region, which was located in the right SNpc, was significantly correlated with the SUVR values of the right posterior putamen. This suggests that the ROIs located in the right N1 regions of patients with PD, which was determined using a voxel-wise analysis, may not fully reflect the status of DAT activity in the ipsilateral posterior putamen. The larger ROI mirrored from the left N1 region may more accurately reflect the status of DAT activity in the posterior putamen.

While significant correlations were found between the CR values of the left and flipped-left N1 regions and the SUVR values in the bilateral posterior putamen on ¹⁸F-FP-CIT PET in our study, the correlation coefficients were only moderate (0.288 and 0.363 on the right and left, respectively). A previous study suggested that DAT imaging reflects the dopaminergic phenotype and neuronal dysfunction, with NM-MRI reflecting a structure or neurodegeneration.⁸ It has been shown that loss of DAT activity in the striatum occurs more than the loss of dopaminergic neurons in the SNpc.^{19,20} These discrepant

changes in DAT activity in the striatum and the number of dopaminergic neurons in patients with PD might explain the relatively modest correlations observed in our study.

In this study, the CR values of the ROI in the left N2 region were significantly correlated with the SUVR values of the ipsilateral anterior putamen, which has not been reported previously. In PD, N1 has been found to be affected the most significantly, followed by N2.²¹ ¹⁸F-FP-CIT PET of PD patients has revealed that the posterior putamen is most significantly involved, followed by the anterior putamen and posterior caudate nucleus.²² As the ROIs in the N1 and N2 regions were larger on the left in a previous study,¹⁰ the left SNpc might be more affected in patients. The significant correlations between the CR values of the left N2 region and the SUVR values of the left anterior putamen may therefore be partly due to the more affected left SNpc. This was supported by the results on the clinically more affected, where the SUVR values of both the anterior and posterior putamina were significantly correlated with the CR values of the more-affected N1 region, the more-affected combined N1 and N2 regions, and the more-affected whole SNpc.

In this study, we did not observe a relationship between the CR values of the SNpc and clinical severity based on UPDRS III scores. This was expected since the CR values of the SNpc were not correlated with disease duration in a previous study.¹⁰ Only enrolling patients with early-stage PD might have been responsible for no significant correlation being observed in our study. A significant correlation between the CR values of the SNpc and the UPDRS III scores might appear if patients with both early- and advanced-stage PD are enrolled. However, this was beyond the scope of this study, and so needs to

be assessed in the future.

This was a single-center study that used a specific NM-MRI sequence based on 3D T1-weighted SPACE imaging with DANTE preparation. Although a recent study that used a similar sequence indicated its clinical utility when compared with conventional 3D T1-weighted GRE imaging with magnetization transfer contrast,¹⁶ this specific sequence was only available from a specific MR vendor. This may reduce the generalizability of our results to clinical applications or to research investigations.

In summary, using a specific ROI in the SNpc, this study found significant correlations between the CR values in the SNpc on NM-MRI and the SUVR values in the posterior putamen on ¹⁸F-FP-CIT PET on both sides. On the clinically more affected side, there were significant correlations between the CR values in the SNpc on NM-MRI and the SUVR values in the anterior and posterior putamina on ¹⁸F-FP-CIT PET.

Supplementary Materials

The online-only Data Supplement is available with this article at <https://doi.org/10.3988/jcn.2022.0147>.

Availability of Data and Material

The datasets generated or analyzed during the study are available from the corresponding author on reasonable request.

ORCID iDs

Seongbeom Park	https://orcid.org/0000-0002-0759-6826
Young Hee Sung	https://orcid.org/0000-0002-2840-1338
Woo Ram Kim	https://orcid.org/0000-0003-1361-4426
Young Noh	https://orcid.org/0000-0002-9633-3314
Eung Yeop Kim	https://orcid.org/0000-0002-9579-4098

Author Contributions

Conceptualization: Seongbeom Park, Eung Yeop Kim. Data curation: Young Hee Sung, Young Noh. Formal analysis: Seongbeom Park, Eung Yeop Kim. Funding acquisition: Young Hee Sung, Young Noh, Eung Yeop Kim. Investigation: Seongbeom Park, Woo Ram Kim, Eung Yeop Kim. Methodology: Eung Yeop Kim. Project administration: Eung Yeop Kim. Resources: Young Hee Sung, Young Noh. Software: Seongbeom Park. Supervision: Eung Yeop Kim. Validation: Seongbeom Park, Eung Yeop Kim. Visualization: Seongbeom Park, Eung Yeop Kim. Writing—original draft: Seongbeom Park. Writing—review & editing: Seongbeom Park, Young Hee Sung, Eung Yeop Kim.

Conflicts of Interest

The authors have no potential conflicts of interest to disclose.

Funding Statement

This study was supported by the National Research Foundation of Korea (NRF) grants funded by the Korea government (MSIT) (No. 2021R1C1C1003676, 2022R1F1A1073551) and a grant of the Korea Healthcare Technology R&D Project through the Korea Health Industry Development Institute (KHIDI), funded by the Ministry of Health & Welfare, Republic of Korea (grant No: HI14C1135).

REFERENCES

- Colloby SJ, McParland S, O'Brien JT, Attems J. Neuropathological correlates of dopaminergic imaging in Alzheimer's disease and Lewy body dementias. *Brain* 2012;135(Pt 9):2798-2808.
- Kraemmer J, Kovacs GG, Perju-Dumbrava L, Pirker S, Traub-Weidinger T, Pirker W. Correlation of striatal dopamine transporter imaging with post mortem substantia nigra cell counts. *Mov Disord* 2014;29:1767-1773.
- Wang X, Zhang Y, Zhu C, Li G, Kang J, Chen F, et al. The diagnostic value of SNpc using NM-MRI in Parkinson's disease: meta-analysis. *Neurol Sci* 2019;40:2479-2489.
- Cho SJ, Bae YJ, Kim JM, Kim D, Baik SH, Sunwoo L, et al. Diagnostic performance of neuromelanin-sensitive magnetic resonance imaging for patients with Parkinson's disease and factor analysis for its heterogeneity: a systematic review and meta-analysis. *Eur Radiol* 2021;31:1268-1280.
- Cassidy CM, Zucca FA, Girgis RR, Baker SC, Weinstein JJ, Sharp ME, et al. Neuromelanin-sensitive MRI as a noninvasive proxy measure of dopamine function in the human brain. *Proc Natl Acad Sci U S A* 2019;116:5108-5117.
- Kuya K, Shinohara Y, Miyoshi F, Fujii S, Tanabe Y, Ogawa T. Correlation between neuromelanin-sensitive MR imaging and 123I-FP-CIT SPECT in patients with parkinsonism. *Neuroradiology* 2016;58:351-356.
- Isaias IU, Trujillo P, Summers P, Marotta G, Mainardi L, Pezzoli G, et al. Neuromelanin imaging and dopaminergic loss in Parkinson's disease. *Front Aging Neurosci* 2016;8:196.
- Martín-Bastida A, Lao-Kaim NP, Roussakis AA, Searle GE, Xing Y, Gunn RN, et al. Relationship between neuromelanin and dopamine terminals within the Parkinson's nigrostriatal system. *Brain* 2019;142:2023-2036.
- Wengler K, He X, Abi-Dargham A, Horga G. Reproducibility assessment of neuromelanin-sensitive magnetic resonance imaging protocols for region-of-interest and voxelwise analyses. *Neuroimage* 2020;208:116457.
- Sung YH, Noh Y, Kim EY. Early-stage Parkinson's disease: abnormal nigrosome 1 and 2 revealed by a voxelwise analysis of neuromelanin-sensitive MRI. *Hum Brain Mapp* 2021;42:2823-2832.
- Hoehn MM, Yahr MD. Parkinsonism: onset, progression and mortality. *Neurology* 1967;17:427-442.
- Goetz CG, Tilley BC, Shaftman SR, Stebbins GT, Fahn S, Martinez-Martin P, et al. Movement Disorder Society-sponsored revision of the Unified Parkinson's Disease Rating Scale (MDS-UPDRS): scale presentation and clinimetric testing results. *Mov Disord* 2008;23:2129-2170.
- Cho J, Noh Y, Kim SY, Sohn J, Noh J, Kim W, et al. Long-term ambient air pollution exposures and brain imaging markers in Korean adults: the Environmental Pollution-Induced Neurological Effects (EPINEF) study. *Environ Health Perspect* 2020;128:117006.
- Gho SM, Liu C, Li W, Jang U, Kim EY, Hwang D, et al. Susceptibility map-weighted imaging (SMWI) for neuroimaging. *Magn Reson Med* 2014;72:337-346.
- Nam Y, Gho SM, Kim DH, Kim EY, Lee J. Imaging of nigrosome 1 in substantia nigra at 3T using multiecho susceptibility map-weighted imaging (SMWI). *J Magn Reson Imaging* 2017;46:528-536.
- Oshima S, Fushimi Y, Okada T, Nakajima S, Yokota Y, Shima A, et al. Neuromelanin-sensitive magnetic resonance imaging using DANTE pulse. *Mov Disord* 2021;36:874-882.
- Tziortzi AC, Haber SN, Searle GE, Tsoumpas C, Long CJ, Shotbolt P, et al. Connectivity-based functional analysis of dopamine release in the striatum using diffusion-weighted MRI and positron emission tomography. *Cereb Cortex* 2014;24:1165-1177.
- Diedrichsen J, Balsters JH, Flavell J, Cussans E, Ramnani N. A probabilistic MR atlas of the human cerebellum. *Neuroimage* 2009;46:39-46.

19. Caminiti SP, Presotto L, Baroncini D, Garibotto V, Moresco RM, Gianolli L, et al. Axonal damage and loss of connectivity in nigrostriatal and mesolimbic dopamine pathways in early Parkinson's disease. *Neuroimage Clin* 2017;14:734-740.
20. Fazio P, Svenningsson P, Cselényi Z, Halldin C, Farde L, Varrone A. Nigrostriatal dopamine transporter availability in early Parkinson's disease. *Mov Disord* 2018;33:592-599.
21. Damier P, Hirsch EC, Agid Y, Graybiel AM. The substantia nigra of the human brain. II. Patterns of loss of dopamine-containing neurons in Parkinson's disease. *Brain* 1999;122(Pt 8):1437-1448.
22. Oh M, Kim JS, Kim JY, Shin KH, Park SH, Kim HO, et al. Subregional patterns of preferential striatal dopamine transporter loss differ in Parkinson disease, progressive supranuclear palsy, and multiple-system atrophy. *J Nucl Med* 2012;53:399-406.